

Tandem Mass Tag Proteomic Analysis of *in Vitro* and *in Vivo* Models of Cutaneous Leishmaniasis Reveals Parasite-Specific and Nonspecific Modulation of Proteins in the Host

Fernanda Negrão,^{*,†,‡,§} Jolene K. Diedrich,[†] Selma Giorgio,[‡] Marcos N. Eberlin,[§] and John R. Yates III[†]

[†]Department of Chemical Physiology, The Scripps Research Institute, 10550 North Torrey Pines Road, SR302, La Jolla, California 92037, United States

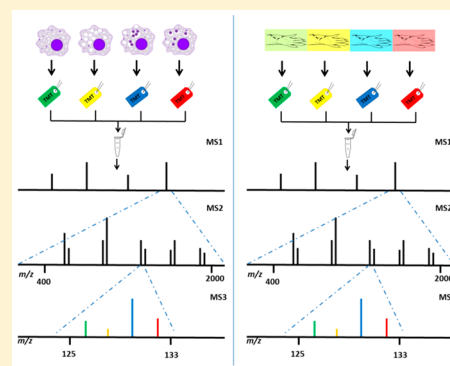
[‡]Department of Animal Biology, Institute of Biology, Rua Monteiro Lobato, 255, Campinas, São Paulo 13083-862, Brazil

[§]School of Engineering, Mackenzie Presbyterian University, Rua da Consolação, 930, São Paulo, São Paulo 01302-907, Brazil

Supporting Information

ABSTRACT: Cutaneous leishmaniasis, the most common form of leishmaniasis, is endemic in several regions of the world, and if not treated properly, it can cause disfiguring scars on the skin. *Leishmania* spp. infection causes an inflammatory response in its host, and it modulates the host metabolism differently depending on the *Leishmania* species. Since *Leishmania* spp. has begun to develop resistance against current therapies, we believe efforts to identify new possibilities for treatment are critical for future control of the disease. Proteomics approaches such as isobaric labeling yield accurate relative quantification of protein abundances and, when combined with chemometrics/statistical analysis, provide robust information about protein modulation across biological conditions. Using a mass spectrometry-based proteomics approach and tandem mass tag labeling, we have investigated protein modulation in murine macrophages (*in vitro* model) and skin biopsies after exposure to *Leishmania* spp. (*in vivo* murine model). Infections induced by *L. amazonensis* (endemic in the New World) and *L. major* (endemic in the Old World) were compared to an inflammation model to search for *Leishmania*-specific and nonspecific protein modulation in the host. After protein extracts obtained from *in vitro* and *in vivo* experiments were digested, the resulting peptides were labeled with isobaric tags and analyzed by liquid chromatography-MS (LC-MS). Several proteins that were found to be changed upon infection with *Leishmania* spp. provide interesting candidates for further investigation into disease mechanism and development of possible immunotherapies.

KEYWORDS: cutaneous leishmaniasis, isobaric labeling proteomics, mass spectrometry, TMT



The leishmaniasis are a group of diseases that can be caused by more than 20 different species of protozoa of the genus *Leishmania*. The disease is transmitted through the bite of sandflies of the genus *Lutzomyia* spp.¹ The three main clinical forms of leishmaniasis are cutaneous, visceral, and mucocutaneous. Cutaneous leishmaniasis (CL) is the most common form of the disease, which usually produces ulcers on the exposed parts of the body, such as the face, arms, and legs.²

It is estimated that up to 1.2 million new CL cases occur each year.³ CL is primarily found in Afghanistan, Algeria, Colombia, Brazil, Iran, Syria, Ethiopia, North Sudan, Costa Rica, and Peru.^{3,4} CL is classified as New World cutaneous leishmaniasis (NWCL) if it is found in the Americas or Old World cutaneous leishmaniasis (OWCL) when it occurs in the Middle East, Mediterranean littoral, Arabian Peninsula, Africa, and India. OWCL typically presents as chronic, painless ulcers or nodules.⁵ Cutaneous leishmaniasis is being spread to the New World due to travel from endemic areas.⁶ In this work, we investigated *Leishmania amazonensis* (*L. amazonensis*; endemic

in the New World⁷) and *Leishmania major* (*L. major*; endemic in the Old World).^{1,3,5}

CL treatment is complex, and the therapy used depends on both the *Leishmania* species causing the infection and where the infection was acquired.⁸ Successful treatment seeks to heal the infection before it becomes chronic, to avoid disfiguring lesions/scars and to decrease the spread of the disease. Typically, treatment involves the parenteral administration of pentavalent antimonials, although there may be alternative or complementary local treatments.⁵ Interestingly, Old World cutaneous leishmaniasis can heal spontaneously but may also respond well to pentavalent antimonials.⁸ However, treatment of New World cutaneous leishmaniasis requires systemic treatment with pentavalent antimonials and is sometimes combined with antibiotics due to the development of parasite

Received: July 24, 2019

Published: October 10, 2019

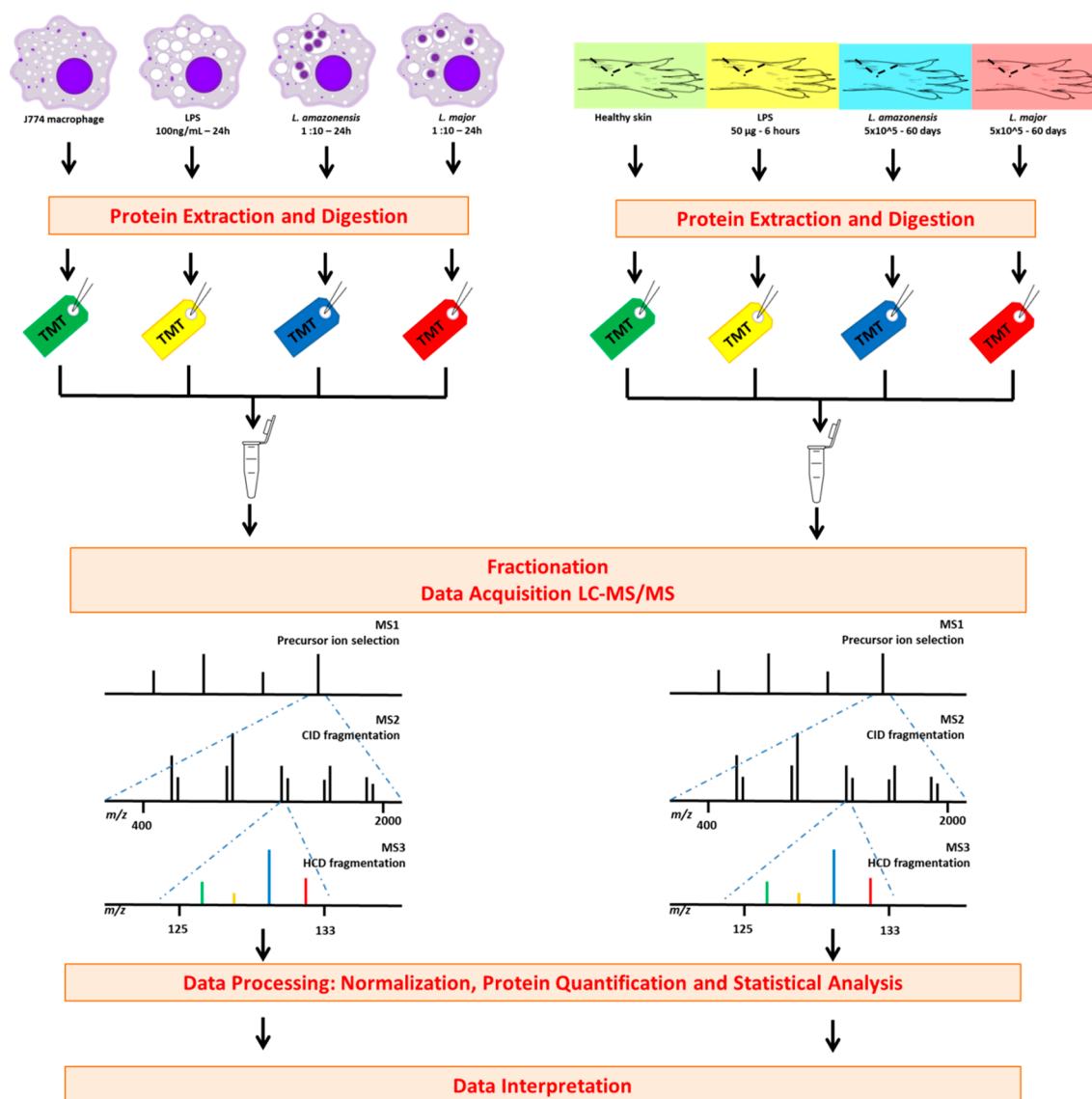


Figure 1. TMT labeling workflow of *in vitro* and *in vivo* experiments. The protocol involves extraction of proteins from cells or tissues followed by reduction, alkylation, and digestion. Samples from each biological condition were labeled with one of the four isobaric tags of the TMT reagent. Resulting peptides were pooled at equal concentrations before fractionation and data acquisition. The TMT-labeled samples were analyzed by LC-MS/MS. In an MS1 scan, same-sequence peptides from the different samples appear as a single unresolved additive precursor ion. Fragmentation of the precursor ion during MS/MS (MS2) yields sequence-informative *b*- and *y*-ions, and further fragmentation by MS3 (SPS) provides quantitative information as distinct masses between *m/z* 126 and 131 representing the four reporter ions. The reporter ion intensity indicates the relative amount of peptide in the mixture that was labeled with the corresponding reagent. Data processing and data interpretation followed data acquisition.

resistance against antimonials.^{8–10} Indeed, previous reports from our group have demonstrated that disease progression and infectivity caused by *L. amazonensis* is more severe than *L. major*.^{11–14}

Recent transcriptomics,¹⁵ lipidomics,^{16,17} and proteomics^{18–21} studies have demonstrated how different species of *Leishmania* modulate the host in order to survive and proliferate.²² Our most recent studies^{13,23} compared an inflammation model to different species of *Leishmania* spp. to reveal hundreds of *Leishmania*-specific proteins that are modulated in the host.

Mass spectrometry-based proteomics²⁴ and machine learning algorithms²⁵ have been combined to produce a powerful tool to perform fast and accurate screening of biological samples. In this study, we performed tandem mass tag (TMT)

labeling proteomics for both *in vitro* and *in vivo* experiments. Our results confirm previous transcriptomics/proteomic findings and extend our understanding of protein modulation in the host after *L. amazonensis* or *L. major* infection. Interestingly, the upstream analysis of interleucin-10 receptors (ILRA10) and the isoform 3 of stimulator of interferon genes protein (Tmem173) revealed enhanced activation in *Leishmania*-induced macrophages and cutaneous lesions. Moreover, this analysis revealed other proteins that may be interesting candidates for further investigation. Any new treatment that targets *Leishmania* will eventually become ineffective because the parasite's genome plasticity²⁶ allows it to continuously develop resistance to available treatments. However, we believe that understanding the modulation of host proteins during infection will contribute to the development of new therapies

to restore the host's metabolism/immune system and, therefore, to eliminate the parasite.

■ RESULTS AND DISCUSSION

Leishmania-Mediated Modulation of Host Protein Expression. Previous transcriptomic and proteomic reports have demonstrated *Leishmania*-induced regulation of gene/protein expression in infected cells/tissues and have attempted to correlate such responses to disease outcome.^{18,20,27–30} These reports confirm that *Leishmania* induces host cells to change their metabolism to guarantee parasite survival and that some of these changes depend on the species of the parasite causing the infection. The understanding of the parasite–host relationship is fundamental for the development of therapeutic tools to control parasitic infections, and *Leishmania* is no exception. In this study, we used mass spectrometry-based proteomics to evaluate *Leishmania*-specific protein modulation in macrophages and in cutaneous tissue. Promastigotes of *L. amazonensis* and *L. major* primarily infect macrophages where they differentiate into amastigotes and multiply inside of the cells. As recently published by our group, *in vitro* experiments were monitored through microscopy, and it was shown that *L. amazonensis* and *L. major* had successfully infected J774 macrophages within 24 h of infection.¹³ Likewise, *in vivo* experiments were monitored by measuring footpad enlargement caused by the infection/inflammation over time, and by 60 days post-infection, both species had caused footpad enlargement of at least 30% and had revealed signs of necrosis.²³ *In vitro* and *in vivo* assays, protein extraction, and digestion were performed as previously described.^{13,23} The following sections describe our findings on the modulation of proteins in the host (macrophages and mice) following *Leishmania* infection or LPS stimulation. Some of our previous work has demonstrated that infection caused by *L. amazonensis* induces the formation of strongly vacuolized macrophages, each of them containing multiple amastigotes,¹³ and that infection by *L. amazonensis* progresses more aggressively than infection caused by *L. major*.^{12,23,31} The correlation between the results from *in vitro* and *in vivo* infections should not be discarded since both were induced by promastigotes of *Leishmania* spp. that turn into amastigotes inside of the macrophages after a few hours. **Figure 1** represents the workflows employed to achieve the relative quantification of proteins in *in vitro* and *in vivo* experiments using tandem mass tag (TMT) labeling, an isobaric labeling-based relative quantification technique used in shotgun proteomics. TMT tags react with the ϵ -amino group of lysine to form an amide linkage that fragments when subjected to collision-induced dissociation. This labeling is efficient for all peptides regardless of protein sequence.³²

TMT technology allows comparative analysis of multiple experiments upon perturbation and is immune to missing values that affect identification and quantification. When samples are run separately as in label-free quantification methods, an ion selected for fragmentation in one LC–MS/MS run may not be selected in subsequent runs or the spectra may not be acquired, which results in missing values. However, in isobaric labeling quantification, all labeled samples have a common precursor ion corresponding to the same peptide species which is fragmented to yield quantitative information across samples within a single experiment. TMT technology is useful to search for the modulation of proteins in the host after

the exposure to different species of *Leishmania* when compared to an inflammation model.

For TMT labeling-based quantification, each sample was derivatized with an isotopic variant of a TMT reagent, and then, the samples were pooled and analyzed simultaneously in a mass spectrometer. The fragmentation of the precursor ion during MS/MS resulted in peptide fragment ion peaks that are used for identification of the peptide and, subsequently, the proteins. Further fragmentation by MS3 allows accurate quantification of the identified proteins. Since all tryptic peptides can be labeled in an isobaric labeling experiment, more than one peptide representing the same protein may be identified, thereby decreasing missing values between experiments and increasing the confidence in both the identification and quantification of the protein.

Leishmania-Specific Protein Modulation in Macrophages. Using a label-free proteomic approach, our group first demonstrated that macrophages uniquely change their protein expression after *Leishmania* infection.¹³ In summary, we have demonstrated how the parasite *Leishmania* modulates protein expression in infected macrophages differently than in an inflammation model, including identification of proteins modulated exclusively after *Leishmania* exposure and several examples of species-specific modulation of proteins. “*Leishmania*-specific” refers to proteins that were uniquely modulated after *Leishmania* spp. infection and “species-specific” refers to proteins that were differently modulated after *L. amazonensis* or *L. major* infection. While many of the proteins that were quantified by label-free or isobaric labeling in our previous works^{13,23} overlapped, others were uniquely observed using only one methodology. Thus, the results were complementary. However, since isobaric labeling is more accurate and efficient, we performed proteomics using isobaric labeling to search for alterations in protein expression in macrophages following *Leishmania amazonensis* or *Leishmania major* infection and compared the results with an inflammation model (LPS stimulation) to search for *Leishmania*-specific protein modulation. A total of four conditions were analyzed: healthy macrophage (i), LPS stimulated macrophage (ii), and *L. amazonensis* or *L. major* infected macrophages (iii and iv, respectively). Experiments were conducted in biological triplicates. Proteins were extracted, digested, and labeled with a TMT tag. The four conditions were pooled, and the data were acquired using an Easy 1000 LC coupled to an Orbitrap Fusion mass spectrometer (Thermo Fisher Scientific, Bremen, Germany).

Table S1 shows the total number of identified peptides and proteins and the peptide/protein ratio for each sample. We applied principal component analysis (PCA), an unsupervised multivariate analysis, to find trends in the data set. Our results showed that 78.1% of variance is observed at the first two principal components (PCs) (**Figure S1**). The first PC explains the differences between healthy and stimulated (infection or inflammation) macrophages. The clustering of the data from *Leishmania* spp. infections and the inflammation model shows the high degree of similarity among them. Therefore, a heatmap with hierarchical clustering analysis was employed as another tool to evaluate clustering of the data set. **Figure S2** reveals successful clustering of samples according to the 30 most statistically significant proteins based on their corrected *p*-values (FDR). Upregulation of cyclin-dependent kinase 1 (P11440), equilibrative nucleoside transporter 1 (Q9JIM1), 60S acidic ribosomal protein P2 (P99027), ribonucleoside

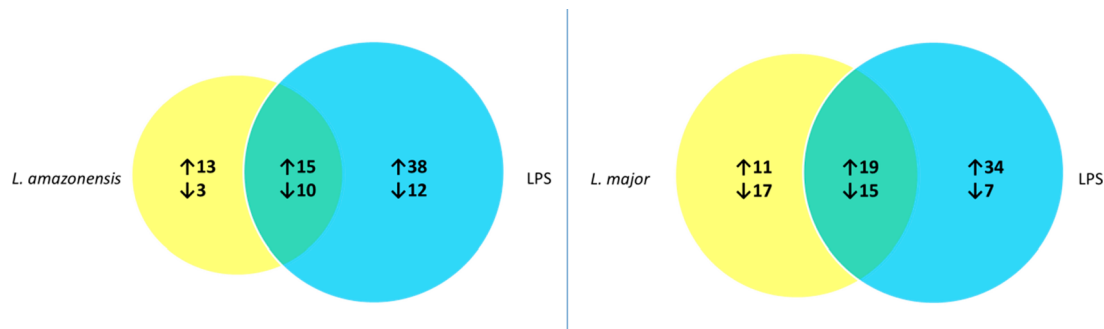


Figure 2. Venn diagrams represent the number of altered proteins (arrows represent the number of up- and downregulated proteins) for each comparison. (Left) Healthy macrophages versus *L. amazonensis* infection (yellow) and healthy macrophages versus inflammation (blue). (Right) Healthy macrophages versus *L. major* infection (yellow) and healthy macrophages versus inflammation (blue). The proteins that were found in common between the infection and inflammation showed the same modulation (i.e., if it was upregulated after inflammation, it was upregulated after infection).

diphosphate reductase large subunit (P07742), cytosine-5 methyl transferase 1 (P13864), and importin subunit alpha-1 (PS2293) was observed after *Leishmania* spp. infections. The loading plots of proteins P99027, P07742, and P13864 can be clearly seen in Figure S1B, indicating their contributions to cluster samples.

t tests were performed on the data set as a univariate analysis to reject the null hypothesis when measuring the relative abundance of proteins after macrophages are exposed to *Leishmania* spp. or LPS. Fold changes were independently calculated to measure changes in protein abundance after macrophages were exposed to *Leishmania* spp. or LPS. Tmem 173 (Uniprot ID: P40240) was the most upregulated protein in macrophages after both *Leishmania* infections, so it was selected for Western blot to validate protein quantification (Figure S3). Moreover, upstream analysis from cutaneous lesions indicated Tmem173 activation (*vide Leishmania*-Specific Protein Modulation in Cutaneous Lesions).

The number of altered proteins in healthy macrophages versus infection (yellow) and versus inflammation (blue) are represented in Venn diagrams (Figure 2). Some protein IDs and their modulations will be discussed below. The complete table of modulated proteins is available as Supporting Information.

We also looked at species-specific protein modulation in infected macrophages. A total of 71 proteins were found to be statistically significant. Nine and 30 proteins of these were exclusively modulated following *L. amazonensis* and *L. major* infection, respectively; 32 were found in common sharing the same modulation (Figure 3).

The proteins that showed the greatest fold changes in expression in macrophages after *Leishmania* infection were also observed to change in the inflammation model (except for Mtpap, which was only upregulated after the infections). However, Tmem41b and Cyb5r4 seemed to be specific to each species of *Leishmania* (Table 1, in bold). The complete table of modulated proteins is available as Supporting Information.

Tmem41b was upregulated after *L. amazonensis* infection and LPS stimulation, and no change was observed after *L. major* infection. Tmem41b was recently addressed as an ER transmembrane protein required for autophagosome biogenesis and lipid mobilization.³³ Moreover, Tmem41b is physically and functionally associated with vacuole membrane protein 1, which promotes the formation of intracellular vacuoles,³⁴ and this association could be related to the

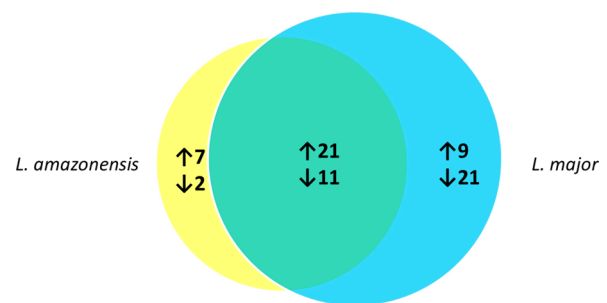


Figure 3. Venn diagram represents the number of altered proteins (arrows represent the number of up- and downregulated proteins) in macrophages comparing infections caused by *L. amazonensis* (yellow) or by *L. major* (blue). The proteins found in common between the infections showed the same modulation (i.e., if it was upregulated after *L. amazonensis* exposure, it was upregulated after *L. major* exposure).

Table 1. List of the Most Altered Proteins According to Fold Changes in Macrophages after Stimulation by *Leishmania* spp. Compared to LPS^a

Uniprot ID	gene	protein name	FC ^b		
			LA ^c	LM ^d	LPS ^e
Q8K1A5	Tmem41b	transmembrane protein 41B	3.2	–	3.2
Q3TDX8	Cyb5r4	cytochrome b5 reductase 4	–	11.2	11.2
Q3TBT3-3	Tmem173	isoform 3 of stimulator of interferon genes protein	11.4	11.2	12.4
Q9D0D3	Mtpap	poly(A) RNA polymerase, mitochondrial	10.6	10.3	–

^aBlanks (–) represent that protein modulation was not statistically significant. ^bFC: fold change. ^cLA: *L. amazonensis* infected macrophage. ^dLM: *L. major* infected macrophage. ^eLPS: lipopolysaccharide stimulated macrophage.

formation of large and communal vacuoles harboring *L. amazonensis*.

Cyb5r4 is an enzyme that exhibits NADPH-hemoprotein reductase activity, which is involved in NADP metabolic processes. Cyb5r4 was 11× upregulated after *L. major* infection and LPS stimulation, and no change was observed after *L. amazonensis* infection. Tmem173 encodes a protein known

as *sting*, which stimulates the immune response through beta-interferon synthesis, a cytokine that promotes inflammation.³⁵ *Leishmania* spp. and LPS induce inflammatory processes, and Tmem173 was significantly upregulated in macrophages upon exposure. Mtpap, a mitochondrial RNA polymerase, plays a role in replication-dependent histone mRNA degradation. Mtpap may be involved in the terminal uridylation of mature histone mRNAs before their degradation is initiated.³⁶ It is significantly upregulated after *Leishmania* spp. infections but not after inflammation, indicating that the expression of Mtpap is specifically related to leishmaniasis.

Furthermore, IPA upstream analysis predicts the inhibition of IL-10 receptors (IL10RA) through the upregulation of aconitate decarboxylase 1 (ACOD1), toll-like receptor 2 (TLR2), solute carrier family 2 member 1 (SLC2A1), and solute carrier family 7 member 11 (SLC7A11) genes after *Leishmania* spp. infections in macrophages (Figure 4). IL-10 is

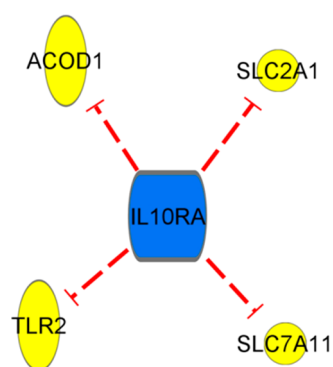


Figure 4. Upregulation of ACOD1, TLR2, SLC2A1, and SLC7A11 after *Leishmania* spp. infections in macrophages predicted the inhibition of IL10RA.

an important regulatory cytokine involved in parasite control in leishmaniasis; it directly suppresses effects on T cell responses, and it has been shown to lead to parasite persistence.³⁷ Our results demonstrate the inhibition of IL-10 receptors at 24 h post-infection, an indication of disease progression that suggests that stimulation of IL10RA may be an interesting approach to control the infection (Table 2). We encourage

Table 2. Upstream Analysis of Macrophages after *Leishmania* spp. Infection

upstream regulator	molecule type	predicted activation state	activation z-score	target molecules in data set
IL10RA	transmembrane receptor	inhibited	-2000	ACOD1, SLC2A1, SLC7A11, TLR2

further research using targeted approaches such as gene knockout experiments and/or adding drug inhibitors/enhancers of selected proteins to evaluate the control of the disease.

Leishmania-Specific Protein Modulation in Cutaneous Lesions. Our previous label-free proteomics results revealed differences in protein expression in skin biopsies after *Leishmania* or LPS exposure.²³ To improve the accuracy of protein quantification, we performed an isobaric labeling proteomic approach to search for alterations in protein

expression in skin biopsies following *Leishmania* spp. infection or inflammation (LPS stimulation). A total of four conditions were analyzed in biological quintuplicates (healthy skin from footpads (i), inflammation induced by LPS (ii), and lesions induced by *L. amazonensis* or *L. major* (iii and iv, respectively)).

Table S2 shows the total number of identified peptides and proteins and the peptide/protein ratio for each sample; it also demonstrates data reproducibility. PCA was used to cluster samples in an unsupervised manner and showed that 69% of variance is explained by the first two principal components (PCs) (Figure S5). The first PC essentially explains the differences between the four different conditions. However, the greatest differences are observed between the clustering of the control group and the inflammation model (i) and the control group and *Leishmania* spp. infections (ii). Therefore, a heatmap with hierarchical clustering analysis was employed as another tool to evaluate clustering of the data set. Figure S6 reveals successful clustering of samples according to the 50 most statistically significant proteins based on their corrected *p*-values (FDR). This analysis shows that, after *Leishmania* spp. infections, 45 proteins of the 50 observed proteins were upregulated. The loading plots of some of these proteins are shown in Figure S5B.

Univariate analysis using *t* tests was applied to the data set, similar to the analysis of the *in vitro* data set. *p*-values were corrected for multiple comparisons using the Benjamini–Hochberg method to filter out protein identifications with false discovery rates (FDR) greater than 5%. Fold changes were independently calculated to measure changes in protein abundance after macrophages were exposed to *Leishmania* spp. or LPS. Western blot of protein Arg1 was performed to validate protein quantification (Figure S8). Arg1 (Uniprot ID: P40240) was specifically upregulated after *Leishmania* infection when compared to the inflammation model.

The number of altered proteins in healthy macrophages versus infection (yellow) and versus inflammation (blue) were represented in Venn diagrams (Figure 5). Our results revealed that all protein IDs that were shared between infection and inflammation displayed the same modulation. (Protein IDs and their modulations will be discussed in the following sections.) The complete table of modulated proteins is available as Supporting Information.

We also looked at species-specific protein modulation in cutaneous lesions. A total of 482 protein IDs were found to be statistically significant. A total of 203 and 21 proteins of these were exclusively modulated following for *L. amazonensis* and *L. major* infection, respectively; 258 were found in common, sharing the same modulation (Figure 6).

Some of the greatest fold changes in protein expression in cutaneous lesions were also observed in the inflammation model. Protein expression changes seem to be specific to each species of *Leishmania* (Table 3, in *italic*), with the exception of Clec10a, which exhibited opposite modulation in infection and inflammation (Table 3, in **bold**). The complete table of modulated proteins is available as Supporting Information.

Lpcat 1 converts phospholipase A2 back to PC after PC hydrolysis to lysophosphatidylcholine, and elevated levels of lysophosphatidylcholine are known to play a pathogenic role in the inflammatory events.³⁸ However, the role of Lpcat1 in leishmaniasis has not yet been reported. Our results reveal a 2.75× greater upregulation of Lpcat 1 after *Leishmania*

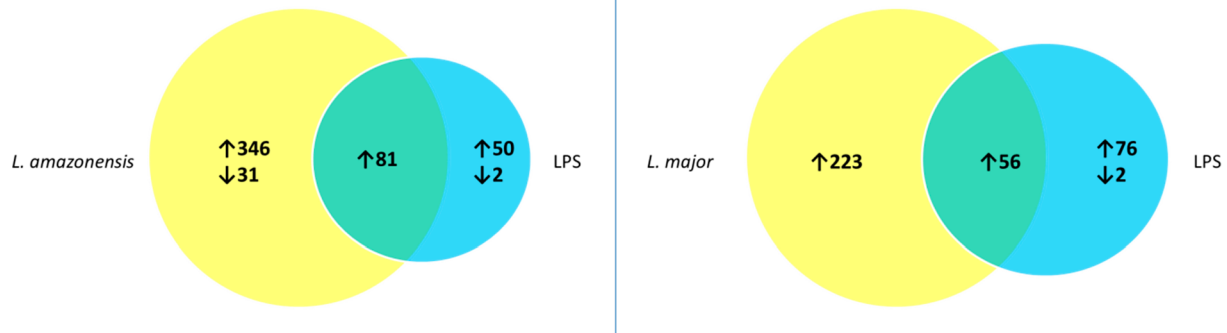


Figure 5. Venn diagrams represent the number of altered proteins (arrows represent the number of up- and downregulated proteins) comparing (Left) healthy skin versus cutaneous lesions induced by *L. amazonensis* (in yellow) and healthy skin versus inflammation (in blue); (Right) healthy skin versus cutaneous lesions induced by *L. major* (in yellow) and healthy skin versus inflammation (in blue). The protein IDs that were found in common between the infection and inflammation showed the same modulation (i.e., if it was upregulated after inflammation it was upregulated after infection).

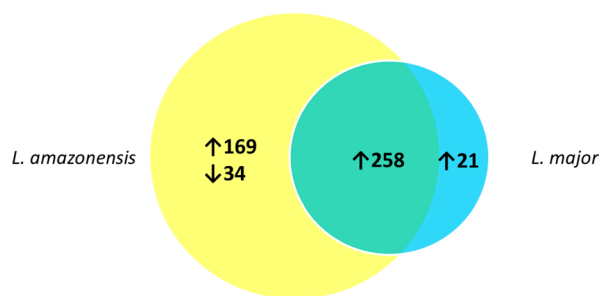


Figure 6. Venn diagrams represent the number of altered proteins comparing lesions induced by *L. amazonensis* (yellow) or by *L. major* (blue). The proteins found in common between the infections showed the same modulation (i.e., if it was upregulated after *L. amazonensis* exposure, it was upregulated after *L. major* exposure).

infection than after LPS stimulation, indicating that *Leishmania* strongly induces the expression of Lpcat1.

The proteoglycan Srgn (serglycin) is important for the binding and storage of proteases within the secretory cytoplasmic granules. Proteoglycans and glycosaminoglycans are involved with inflammatory/immune responses and have been studied for leishmaniasis as potential therapeutic targets.³⁹ Our results revealed that Srgn is specifically >10× upregulated after *Leishmania* infection.

Macrophages, as antigen presenting cells, sense the micro-environment through several types of receptors that recognize pathogen-associated molecular patterns, including C-type lectins receptors. C-type lectins receptors recognize and internalize specific carbohydrate antigens in a Ca²⁺-dependent manner and have been targeted in strategies for parasite recognition.⁴⁰ However, very little is known about how C-type lectins receptors are involved in host–pathogen relationships. Interest in the role of C-type lectins receptors in parasite infections is growing since it impacts our understanding of specific immune responses and, therefore, the outcome of the disease.⁴⁰ The differential regulation of Clec10a after *Leishmania* exposure remains to be validated.

Ttyh3 and Tamm41 are specifically upregulated in cutaneous lesions after *L. amazonensis* and LPS exposure. Ttyh3 (protein tweety homologue 3) is a calcium activated membrane protein with chlorine channel activity,⁴¹ and Tamm41, a mitochondrial phosphatidate cytidylyltransferase, catalyzes the formation of CDP-diacylglycerol from phospho-

tidic acid in the mitochondrial inner membrane. Tamm41 is required for the biosynthesis of cardiolipins that stabilize supercomplexes of the mitochondrial respiratory chain in the mitochondrial inner membrane.⁴² Mmp12, macrophage metalloelastase, is involved in tissue injury and remodeling⁴³ and is only statistically upregulated in cutaneous lesions after *L. amazonensis* exposure.

Lsm1 (U6 snRNA-associated Sm-like protein LSm1) is exclusively upregulated in cutaneous lesions after *L. major* or LPS exposure. Lsm1 plays a role in the degradation of histone mRNAs and is part of an Lsm subunits-containing complex involved in the general process of mRNA degradation.⁴⁴ Heatr3 (HEAT repeat-containing protein 3) is upregulated after *L. major* exposure but not after LPS stimulation. Lsm1 and Heatr3 have not previously been linked to leishmaniasis, but a 6-fold change increase specifically after *L. major* exposure warrants further attention.

Furthermore, IPA upstream analysis predicted the inhibition or activation of several gene products, such as the inhibition of IL-10 receptors (as observed in the *in vitro* results) and activation of p38MAPK and Tmem173 (also observed in the *in vitro* results).

The inhibition of IL10RA was predicted by the upregulation of several proteins (Figure 7A), confirming what was previously observed for the *in vitro* analysis. One of the hypotheses of our previous work was that the activation of p38 MAPKs would be enhanced after *Leishmania* exposure.^{13,23} Indeed, the present study confirms p38 MAPKs activation by the upregulation of six proteins (Figure 7B). Kumar and colleagues had previously demonstrated that selected anti-inflammatory drugs inhibit LPS-stimulated cytokine production, and this was linked to the inhibition of p38 MAPK and, consequently, cytokine synthesis.⁴⁵ Since *Leishmania* exposure enhances p38 MAPKs, it may be possible that these anti-inflammatory drugs can be used to control *Leishmania* infection. Tmem173 encodes a protein known as *sting* that was demonstrated in this work to be activated in macrophages after *Leishmania* exposure (Figure 7C). Further, according to the previously reported results from the *in vitro* analysis (*vide Leishmania-Specific Protein Modulation in Macrophages*), Tmem173 was 10× upregulated in infected macrophages, supporting the hypothesis that the infection could have led to the upregulation of Tmem173 in cutaneous lesions. Table 4 shows all the predicted upstream regulators and reveals protein

Table 3. List of the Most Altered Proteins According to Fold Changes in Skin Biopsies after Stimulation by *Leishmania* spp. Compared to LPS^a

accession	gene	protein name	FC ^b		
			PA ^c	PM ^d	LPS ^e
Q62431	Arid3a	AT-rich interactive domain-containing protein 3A	12.14295	12.31443	2.922205
Q3TFD2	Lpcat1	lysophosphatidylcholine acyltransferase 1	11.8402	11.34467	4.271749
P13609	Srgn	serglycin	10.6886	11.032	–
Q9Z0M6-3	Cd97	isoform 3 of CD97	10.40081	10.8547	7.037561
Q64277	Bst1	ADP-ribosyl cyclase/cyclic ADP-ribose hydrolase 2	10.22397	9.437355	3.080815
P41233	Abca1	ATP-binding cassette subfamily A member 1	9.93927	9.410309	2.851242
Q9Z2X2	Psmd10	26S proteasome non-ATPase regulatory subunit 10	7.404141	8.2042	7.296379
Q3USJ8-3	Fchsd2	isoform 3 of F-BAR and double SH3 domains protein 2	7.261907	7.301614	–
Q9EP73	Cd274	programmed cell death 1 ligand 1	5.081787	4.713175	–
P35174	Stfa2	Stefin-2	4.091948	4.18246	2.706628
A0A0B4J1G0	Fcgr4	low affinity immunoglobulin gamma Fc region receptor IV	3.860301	3.819861	2.271174
P49300	Clec10a	C-type lectin domain family 10 member A	3.757269	3.670073	0.33767
Q80SY3	Atp6v0d2	V-type proton ATPase subunit d 2	3.739901	3.209451	1.253348
Q8BGB5	Limd2	LIM domain-containing protein 2	2.730265	2.813116	1.522233
Q9D8U6	Mcemp1	mast cell-expressed membrane protein 1	2.826001	2.723099	1.763518
P59764	Dock4	dedicator of cytokinesis protein 4	2.77799	2.628505	1.480765
Q61462	Cyba	cytochrome b-245 light chain	2.577298	2.584057	1.395501
P24063	Itgal	integrin alpha-L	2.59674	2.484184	2.086825
Q8VE96	Slc35f6	solute carrier family 35 member F6	2.806858	2.463607	1.703107
P53569	Cebpz	CCAAT/enhancer-binding protein zeta	2.303913	2.240065	1.381253
P12032	Timp1	metalloproteinase inhibitor 1	2.288097	2.204282	1.820899
P97430	Slpi	antileukoprotease	2.088751	2.199712	1.768082
Q8K0B2-3	Lmbrd1	isoform 3 of probable lysosomal cobalamin transporter	2.391046	2.070068	1.427895
Q6PSF7	Ttyh3	protein tweety homologue 3	3.738347	–	3.832628
P34960	Mmp12	macrophage metalloelastase	2.053823	–	–
Q3TUH1	Tamm41	phosphatidate cytidyltransferase, mitochondrial	2.018851	–	1.418603
Q8VC85	Lsm1	U6 snRNA-associated Sm-like protein	–	6.505335	3.175993
Q8BQM4	Heatr3	HEAT repeat-containing protein 3	–	6.364826	–

^aBlanks (–) represent that protein modulation was not statistically significant. ^bFC: fold change. ^cPA: *L. amazonensis* infected macrophage. ^dPM: *L. major* infected macrophage. ^eLPS: lipopolysaccharide stimulated macrophage.

candidates that should be further investigated using targeted approaches, such as immunohistochemistry to add information on protein distribution and/or gene knockout experiments to evaluate the control of the disease.

CONCLUSIONS

Substantial differences in protein expression in *Leishmania* infected macrophages, infected skin, and an inflammation model have been found. As recently reported by our group, some proteins were species-specifically modulated after *Leishmania* spp. exposure, which we believe leads to differences in disease progression. In this work, our findings first revealed the quantification of exclusively modulated proteins after *L. amazonensis* or *L. major* exposure in macrophages. The upregulation of Tmem41b was specific after *L. amazonensis* infection, whereas Cyb5r4 was specifically regulated after *L. major* infection. Tmem173 was nonspecifically upregulated in macrophages (it was upregulated after infections and inflammation), and Mtpap was uniquely upregulated after *Leishmania* spp. infections. IPA upstream analysis predicted the inhibition of IL10RA in infected macrophages, which suggests that targeting this transmembrane could be a potential way to control the infection.

For the murine model of infection, several proteins, such as Lpcat1, Srgn, and Clec10a were exclusively upregulated in cutaneous lesions induced by *Leishmania* compared to the inflammation model. Clec10a was discussed as an interesting

target to be further investigated to explore the host–pathogen relationship. Ttyh3, Tamm41, and Mmp12 were specifically upregulated in cutaneous lesions induced by *L. amazonensis*, whereas Lsm1 and Heatr3 were specifically upregulated in cutaneous lesions induced by *L. major*. Moreover, IPA upstream analysis has also predicted the inhibition of IL10RA as well as the activation of several gene products, such as p38MAPK and Tmem173, that may contribute to a better understanding of the pathogenesis of leishmaniasis. Our findings added relevant information about the host's protein expression following *Leishmania* infection, encouraging further research on selected proteins to deepen the understanding on the *Leishmania*–host relationship.

METHODS

Parasite Cultures. *L. amazonensis*, strain MHOM/BR/67/M2269, and *L. major*, strain Friedlin, were maintained by regular passage in BALB/c mice, in accordance with the Ethics Committee on the Use of Animals number 4041-1 (CEUA/UNICAMP Universidade Estadual de Campinas). *L. amazonensis* and *L. major* promastigotes were kept in RPMI medium containing 10% FBS and gentamicin at 50 µg/mL and pH 7.4. Parasite cultures were maintained at 26 °C. The starter culture contained 10⁵ promastigotes in 5 mL of medium, and the parasites were used for *in vitro* and *in vivo* assays.

In Vitro Assay. The J774 macrophage cell line from BALB/c mice was obtained from the American Type Culture

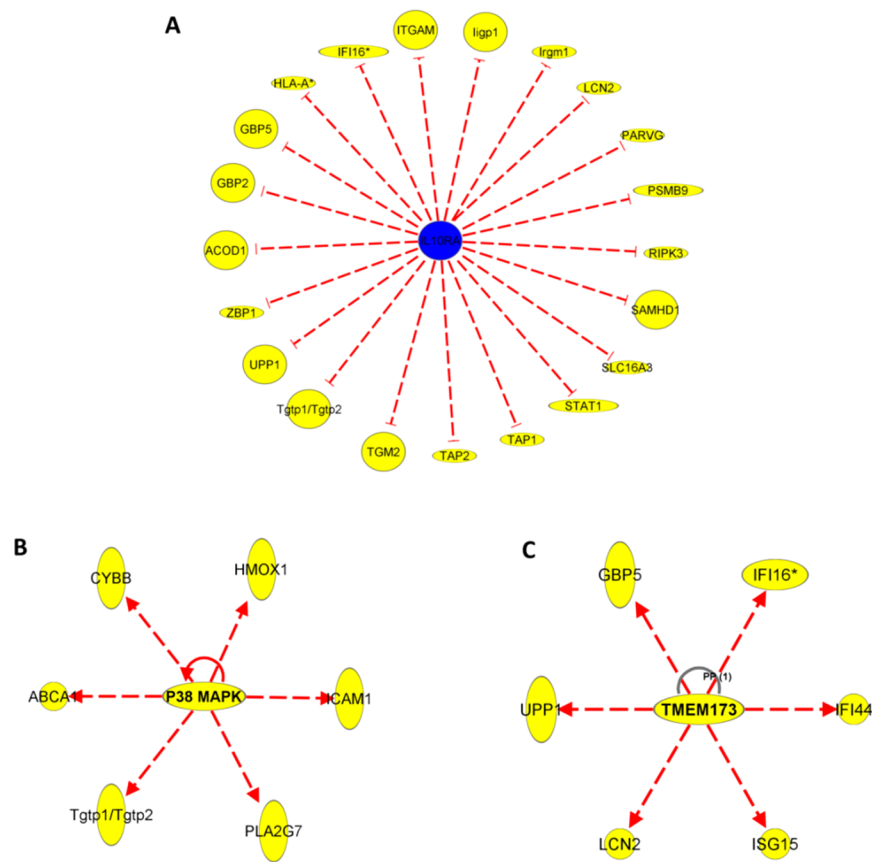


Figure 7. Upregulation of selected proteins in cutaneous lesions after *Leishmania* spp. exposure leads to inhibition of IL10RA (A); activation of p38 MAPK (B), and activation of Tmem173 (C).

Table 4. Upstream Analysis of the Host after *Leishmania* spp. Infection

upstream regulator	molecule type	predicted activation state	activation z-score	target molecules in data set
IL10RA	transmembrane receptor	inhibited	-3965	ACOD1, GBP2, GBP5, HLA-A, IFI16, Iigp1, Irgm1, ITGAM, LCN, NPL, PARVG, PSMB9, RIPK3, SAMHD1, SLC16A3, STAT1, TAP1, TAP2, TGM2, Tgtp1/Tgtp2, TTR, UPP1, ZBP1
APOE	transporter	inhibited	-3434	ABCA1, APOA1, CD44, CD68, CTSB, CTSS, CYBB, FCGR2B, HMOX1, HSD11B1, ICAM1, ITGAM, LCN2, MSR1, NCF1, NCF2, S100A8, S100A9, TIMP1
APOA1	transporter	inhibited	-2236	CYBB, ICAM1, ITGAM, MPO, XDH
P38 MAPK	group	activated	2385	ABCA1, CYBB, HMOX1, ICAM1, PLA2G7, Tgtp1/Tgtp2
IFN alpha/beta	group	activated	2813	CLEC10A, HLA-A, IFI16, Irgm1, SLPI, STAT1, STAT2, Tgtp1/Tgtp2
IL1	group	activated	3512	CRP, CTSB, CTSC, HMOX1, HP, ICAM1, ITGAM, ITGB2, LYZ, S100A9, TGM2, TIMP1, TNC, XDH
Tlr	group	activated	2219	ARG1, HLA-A, ICAM1, LCN2, STAT1
IL33	cytokine	activated	2023	ARG1, ELMO1, EPX, HCK, HMOX, ICAM1, ITIH1, NCF4, PAPSS2, PRG2, S100A8, TIMP1, TNFAIP2
TMEM173	other	activated	2433	GBP5, IFI16, IFI44, ISG15, LCN2, UPP1

Collection. Cells were grown at 37 °C in RPMI medium supplemented with 10% FBS and 50 µg/mL gentamicin in a humidified atmosphere of 5% CO₂. 5 × 10⁶ cells were plated in 6-well plates and maintained for 18 h. Promastigotes were then added to the macrophages at a ratio of 10:1 parasites/cell. *Escherichia coli* lipopolysaccharide (LPS) (Sigma) stimulated macrophages were used as an inflammation model by adding 100 ng/µL LPS to each well for 24 h.⁴⁶ *In vitro* assays were conducted in three replicates for each condition (healthy, LPS stimulated, and infected macrophages). Microscopy analyses were performed to confirm the infection as described elsewhere.¹³

In Vivo Assay. A total of 5 × 10⁶ promastigotes (*L. amazonensis* or *L. major*) were inoculated into the right footpads of 5 week-old female BALB/c mice, obtained from the Centro de Bioterismo/UNICAMP. Experiments were performed in accordance with the Ethics Committee on the Use of Animals number 4041-1 (CEUA/UNICAMP Universidade Estadual de Campinas). The inflammation model was obtained after inoculation of 50 µg of lipopolysaccharide (LPS) solution (1 µg/µL) in the right footpads of mice. Footpads from an uninfected mouse were used as negative controls. Mice were sacrificed by cervical dislocation after 60 days of infection (*L. amazonensis* or *L. major* infection models)

and after the formation of edema induced by LPS inoculation (3 h inflammation model). For proteomic analyses, skin biopsies were obtained from the region right above the walking pads (where LPS and *Leishmania* spp. were inoculated) using a scalpel. The biopsies were snap frozen in liquid N₂ and ground, and proteins were subsequently extracted and digested. The corresponding area was obtained from uninfected footpads as the negative controls. The entire skin biopsy was used to obtain the tissue homogenate so that microenvironment changes might be present. The size of the skin biopsy was not standardized. However, the amount of protein to undergo digestion was calculated as 100 µg per sample. Biological experiments were conducted in three replicates for each condition (healthy, LPS stimulated, and infected footpads). Histology analyses were performed to confirm the infection as described elsewhere.^{11,47}

Peptide Labeling Using Tandem Mass Tags and Data Acquisition. Protein extraction, digestion, and peptide labeling were performed separately for *in vitro* and *in vivo* assays. After determination of protein concentrations using the Pierce BCA Protein Assay Kit (#23225) from Thermo Scientific, a total of 100 µg of protein per sample was aliquoted for digestion. Protein pellets underwent methanol/chloroform precipitation to remove excessive detergents and urea. The recovered pellets were dried completely and then resuspended in 100 µL of 100 mM TEAB (pH 8.5). Proteins were reduced and alkylated as described elsewhere.^{13,23} Proteins were digested by incubation with 1:50 (enzyme/protein, w/w) trypsin overnight at 37 °C with vigorous orbital shaking. Peptides were sequentially quantified using the Pierce for Quantitative Colorimetric Peptide Assay Kit (#23275) from Thermo Scientific. A total of 20 µg of peptide per sample was labeled with tandem mass tag reagent from Thermo Scientific TMT Kit # 90061. TMT reagents were reconstituted according to the manufacturer's instructions. Tubes containing the different isobaric chemical tags (0.8 mg each) were solubilized in 41 µL of anhydrous acetonitrile at room temperature. Reagents were dissolved by vortexing 5 min, and the solutions were gathered by centrifugation. Peptides were labeled by adding 41 µL of TMT isobaric tag, followed by an incubation step for 1 h at room temperature. To quench the reaction, 5% hydroxylamine (8 µL per sample) was added followed by a 15 min incubation at RT. In this four-plex TMT experiment, the biological conditions were finally pooled (healthy (i); inflammation model (ii); *L. amazonensis* infection (iii); *L. major* infection (iv)) into one microtube and then fractionated to 8 fractions using the Pierce High pH Reversed Phase Peptide Fractionation Kit from Thermo Scientific (#84868). Each pooled sample equals one biological replicate. A total of three biological replicates were analyzed for the *in vitro* experiment, whereas five were analyzed for the *in vivo* experiment. Each biological replicate contained 8 fractions that were analyzed in sequence (1–8) by an Easy 1000 coupled to an Orbitrap Fusion Tribid (Thermo Scientific). Samples were eluted on a column self-packed with BEH (Ethylene Bridged Hybrid) (Waters 100 µm inner diameter × 1.7 µm × 20 mm) using a 1–30% gradient of solvent B for 160 min, 30–90% for 60 min, and 90% for 20 min at a 200 µL/min flow rate. Two blanks were run after each biological replicate to avoid carry-over effects.

The Orbitrap Fusion was operated in data-dependent acquisition mode using the Multinotch MS3 method through the XCalibur software.

Survey scan mass spectra were acquired in a positive ion mode in the 400–1500 *m/z* range with the resolution set to 120 000 (fwhm) and AGC target of 4×10^5 on the Orbitrap. The 10 most intense ions per survey scan containing 2–7 charges were selected for CID fragmentation, and the resulting fragments (MS2) were analyzed in the ion trap in the 400–120 *m/z* range. Dynamic exclusion was employed within 10 s to prevent repetitive selection of the same peptide. The 10 most intense MS2 fragments were selected for HCD fragmentation (MS3), and the resulting fragments were detected in the Orbitrap in the 120–500 *m/z* range with the resolution set to 15 000 (fwhm) and AGC target of 10^5 .

Data Processing. Raw files were extracted into ms1, ms2, and ms3 files from raw files using Raw Converter 1.1.0.19 (<http://fields.scripps.edu/rawconv/>). Protein identification was performed using the Integrated Proteomics Pipeline-IP2 (Integrated Proteomics Applications; <http://www.integratedproteomics.com/>) using ProLuCID⁴⁸ and DTASelect2⁴⁹ to a 1% protein false discovery rate (FDR). All tandem mass spectrometry (MS/MS) spectra were compared against the theoretical mass spectra calculated from the *in silico* digested reference database using a decoy strategy.⁵⁰ In order to differentiate between host and *Leishmania* proteins, the MS/MS spectra were searched against a combined database (UniprotKB/*Mus musculus* (mouse); *Leishmania amazonensis*; *L. major* release 2018_04). Only proteins belonging exclusively to the *Mus musculus* database were considered for further analysis. Precursor mass tolerance was set to 50 ppm and fragment ion tolerance, to 600 ppm for CID spectra with mass shifts of 229.1629 *m/z* on lysine/N-terminus and 57.02146 *m/z* (carbamidomethylation) on cysteine as static modifications. PSMs were filtered out for those identifications with a FDR above 1% at the protein level using DTASelect2.⁴⁹

The most intense peptides per survey scan (MS1) were selected for CID fragmentation (MS2) for peptide identification. Next, MS2 fragments were selected for HCD fragmentation (MS3) to release the reporter ions for peptide quantification. Each reporter ion reflects the abundance of a peptide in a sample. The software Census⁵¹ was employed to calculate the relative quantification of proteins at the MS3 level. In brief, the intensity of a given reporter ion was normalized by the sum of the total intensity of all of the reporter ions for each peptide. Thus, the normalized intensities of the reporter ions reflect the relative abundance of a peptide across samples. Next, the normalized abundances of peptides assigned to a given protein were integrated to calculate the relative abundance of proteins.³² For each sample, protein abundances were given as intensities, which were then normalized by the sum of the total intensities of proteins and log transformed to search for *Leishmania*-specific protein modulation in the host.

Statistical Analysis. Statistical analyses were performed separately for the *in vitro* and *in vivo* assays. For the *in vitro*, four conditions were analyzed (healthy macrophage, *L. amazonensis*/*L. major* infected macrophages, and LPS stimulated macrophages), each of them composed of three biological replicates. Likewise, for the *in vivo* samples, four conditions were analyzed (skin biopsy from a healthy footpad, skin lesions induced by *L. amazonensis*/*L. major*, and inflamed skin (LPS)), each of them composed of five biological replicates.

First, the unsupervised multivariate statistical analysis of principal component analyses (PCA) was applied to check for data reproducibility and sample preparation using the online

server MetaboAnalyst 4.0 (www.metaboanalyst.ca).⁵² Then, univariate analysis using the *t* test and fold change calculations were performed to evaluate changes in protein abundance independently to provide descriptive information from “control versus infection” and “control versus inflammation”. Fold change, *p*-values, and corrected *p*-values (FDR) using the Benjamini–Hochberg method were calculated as described elsewhere.^{13,23} Corrected *p*-values < 0.05 were considered statistically significant. Next, heatmaps with Ward’s hierarchical clustering method using the most statistically modulated proteins were accessed for further visualization of the data sets.

Finally, Ingenuity Systems Pathway Analysis v8.8 software (IPA-Ingenuity Systems, Redwood City, CA, USA) was used to predict the upstream regulation of gene products on different conditions. *In vitro* and *in vivo* prediction analyses were performed separately.

Validation of Protein Quantification Using Western Blot Analysis. A total of three lysates for each biological condition were used for the Western blot assays.

For the validation of the *in vitro* protein quantification, the protein Tmem173 was chosen. This protein had an 11-fold increase after infections and a 12-fold increase after inflammation. A total of 20 μ g of lysates was loaded onto a Bolt 4–12% Bis-Tris Plus Gel (Thermo Scientific) and transferred to a nitrocellulose membrane (Thermo Scientific). The proteins were immunostained using anti-Tmem173 antigen (ProteinTech #19851-1-AP) diluted 1:500 with blocking buffer (5% nonfat dry milk in Tris buffered saline with Tween 20 (Sigma-Aldrich)), followed by incubation with the secondary antibody (HRP, Thermo Scientific) diluted 1:5000 with blocking buffer. For the validation of the *in vivo* protein quantification, the protein Arg1 was chosen. A total of 20 μ g of lysates was loaded onto a Bolt 4–12% Bis-Tris Plus Gel (Thermo Scientific) and transferred to a nitrocellulose membrane (Thermo Scientific). ARG1 was upregulated after infections and showed no modulation after the inflammation. First, the proteins were immunostained using anti-ARG1 antigen (from Proteintech-16001-1-AP) diluted 1:1000 with blocking buffer (5% nonfat dry milk in Tris buffered saline with Tween 20 (Sigma-Aldrich)), followed by incubation with the secondary antibody (HRP, Thermo Scientific).

For each primary antibody, Anti-GAPDH (ab181602, Abcam) diluted 1:1000 with blocking buffer was used as a loading control, followed by incubation with a secondary antibody anti-rabbit HRP (ab205718, Abcam) diluted 1:5000 with blocking buffer. ECL Western Blotting Kit (#32106, Thermo Scientific) was used as the chemiluminescence reagent. ImageJ⁵³ was used to access fold change by densitometry (triplicate), and statistical analysis was performed using the Mann–Whitney U Test.

■ ASSOCIATED CONTENT

● Supporting Information

The Supporting Information is available free of charge on the ACS Publications website at DOI: [10.1021/acsinfectdis.9b00275](https://doi.org/10.1021/acsinfectdis.9b00275).

Normalized abundance of all identified proteins across samples; fold changes; original and corrected *p*-values (FDR) for each comparison (XLSX)

Normalized abundance of all identified proteins across samples; fold changes; original and corrected *p*-values (FDR) for each comparison (XLSX)

Table S1, number of identified peptides and proteins and peptide/protein ratio per sample (*in vitro*); Table S2, number of identified peptides and proteins and peptide/protein ratio per sample (*in vivo*); Figure S1, assessment of data quality (principal component analysis); Figure S2, hierarchical clustering with a heatmap for visualization of the data set (*in vitro*); Figure S3, Western blotting of Tmem 173 (*in vitro*); Figure S4, assessment of data quality (principal component analysis); Figure S5, hierarchical clustering with a heatmap for visualization of the data set (*in vivo*); Figure S6, Western blotting of Arg1 (*in vivo*) (PDF)

■ AUTHOR INFORMATION

Corresponding Author

*E-mail: negraosf@gmail.com.

ORCID

Fernanda Negrão: [0000-0002-9839-6511](https://orcid.org/0000-0002-9839-6511)

John R. Yates, III: [0000-0001-5267-1672](https://orcid.org/0000-0001-5267-1672)

Notes

The authors declare no competing financial interest.

■ ACKNOWLEDGMENTS

F.N. and M.N.E acknowledge FAPESP (2017/22651-4). S.G. acknowledges FAPESP 2015/23767-0, and J.R.Y. acknowledges NIH grant P41 GM103533.

■ REFERENCES

- (1) World Health Organization (2016) Leishmaniasis in high-burden countries: an epidemiological update based on data reported in 2014. *Wkly. Epidemiol. Rec.* 91, 285–296.
- (2) WHO (2016) *Leishmaniasis*, WHO, Geneva.
- (3) Alvaiz, J., et al. (2012) Leishmaniasis Worldwide and Global Estimates of Its Incidence. *PLoS One* 7, No. e35671.
- (4) Pigott, D. M., Golding, N., Messina, J. P., Battle, K. E., Duda, K. A., Balard, Y., Bastien, P., Pratlong, F., Brownstein, J. S., Freifeld, C. C., Mekaru, S. R., Madoff, L. C., George, D. B., Myers, M. F., and Hay, S. I. (2014) Global database of leishmaniasis occurrence locations, 1960–2012. *Sci. Data* 1, 140036.
- (5) Heras-Mosteiro, J., Monge-Maillo, B., Pinart, M., Lopez Pereira, P., Reveiz, L., Garcia-Carrasco, E., Campuzano Cuadrado, P., Royuela, A., Mendez Roman, I., and López-Vélez, R. (2017) Interventions for Old World cutaneous leishmaniasis. *Cochrane database Syst. Rev.* 12, CD005067.
- (6) Reithinger, R., Dujardin, J.-C., Louzir, H., Pirmez, C., Alexander, B., and Brooker, S. (2007) Review Cutaneous leishmaniasis. *Lancet Infect. Dis.* 7, 581–596.
- (7) de Vries, H. J. C., Reedijk, S. H., and Schallig, H. D. F. H. (2015) Cutaneous leishmaniasis: recent developments in diagnosis and management. *Am. J. Clin. Dermatol.* 16, 99–109.
- (8) Monge-Maillo, B., and López-Vélez, R. (2013) Therapeutic Options for Old World Cutaneous Leishmaniasis and New World Cutaneous and Mucocutaneous Leishmaniasis. *Drugs* 73, 1889–920.
- (9) Lamotte, S., Späth, G. F., Rachidi, N., and Prina, E. (2017) The enemy within: Targeting host-parasite interaction for antileishmanial drug discovery. *PLoS Neglected Trop. Dis.* 11, e0005480.
- (10) Decuyper, S., Vanaerschot, M., Bruncker, K., Imamura, H., Müller, S., Khanal, B., Rijal, S., Dujardin, J.-C., Coombs, G. H., and Geary, T. G. (2012) Molecular Mechanisms of Drug Resistance in Natural Leishmania Populations Vary with Genetic Background. *PLoS Neglected Trop. Dis.* 6, No. e1514.
- (11) Araujo, A. P., and Giorgio, S. (2015) Immunohistochemical evidence of stress and inflammatory markers in mouse models of cutaneous leishmaniasis. *Arch. Dermatol. Res.* 307, 671–682.

- (12) Negrão, F., de O. Rocha, D. F., Jaeeger, C. F., Rocha, F. J. S., Eberlin, M. N., and Giorgio, S. (2017) Murine cutaneous leishmaniasis investigated by MALDI mass spectrometry imaging. *Mol. BioSyst.* 13, 2036–2043.
- (13) Negrão, F., Fernandez-Costa, C., Zorgi, N., Giorgio, S., Nogueira Eberlin, M., and Yates, J. R. (2019) Label-free proteomic analysis reveals parasite-specific protein alterations in macrophages following *Leishmania amazonensis*, *Leishmania major* or *Leishmania infantum* infection. *ACS Infect. Dis.* 5, 851–862.
- (14) Terreros, M. J. S., de Luna, L. A. V., and Giorgio, S. (2017) Long-term cell culture isolated from lesions of mice infected with *Leishmania amazonensis*: a new approach to study mononuclear phagocyte subpopulations during the infection. *Pathog. Dis.* 75, ftx114.
- (15) Cantacessi, C., Dantas-Torres, F., Nolan, M. J., and Otranto, D. (2015) The past, present, and future of *Leishmania* genomics and transcriptomics. *Trends Parasitol.* 31, 100–108.
- (16) Negrão, F., Abánades, D. R., Jaeeger, C. F., Rocha, D. F. O., Belaz, K. R. A., Giorgio, S., Eberlin, M. N., and Angolini, C. F. F. (2017) Lipidomic alterations of in vitro macrophage infection by *L. infantum* and *L. amazonensis*. *Mol. BioSyst.* 13, 2401–2406.
- (17) Biagiotti, M., Dominguez, S., Yamout, N., and Zufferey, R. (2017) Lipidomics and anti-trypanosomatid chemotherapy. *Clin. Transl. Med.* 6, 27.
- (18) Menezes, J. P. B., Almeida, T. F., Petersen, A. L. O. A., Guedes, C. E. S., Mota, M. S. V., Lima, J. G. B., Palma, L. C., Buck, G. A., Krieger, M. A., Probst, C. M., and Veras, P. S. T. (2013) Proteomic analysis reveals differentially expressed proteins in macrophages infected with *Leishmania amazonensis* or *Leishmania major*. *Microbes Infect.* 15, 579–591.
- (19) Moreira, D. de S., Pescher, P., Laurent, C., Lenormand, P., Späth, G. F., and Murta, S. M. F. (2015) Phosphoproteomic analysis of wild-type and antimony-resistant *Leishmania braziliensis* lines by 2D-DIGE technology. *Proteomics* 15, 2999–3019.
- (20) Singh, A. K., Pandey, R. K., Siqueira-Neto, J. L., Kwon, Y.-J., Freitas-Junior, L. H., Shaha, C., and Madhubala, R. (2015) Proteomic-based approach to gain insight into reprogramming of THP-1 cells exposed to *Leishmania donovani* over an early temporal window. *Infect. Immun.* 83, 1853–68.
- (21) da Silva Santos, C., Attarha, S., Saini, R. K., Boaventura, V., Costa, J., Khouri, R., Barral-Netto, M., Brodskyn, C. I., and Souchelnytskyi, S. (2015) Proteome profiling of human cutaneous leishmaniasis lesion. *J. Invest. Dermatol.* 135, 400–10.
- (22) Rossi, M., and Fasel, N. (2018) How to master the host immune system? *Leishmania* parasites have the solutions! *Int. Immunol.* 30, 103–111.
- (23) Negrão, F., Giorgio, S., Nogueira Eberlin, M., and Yates, J. R. (2019) Comparative Proteomic Analysis of Murine Cutaneous Lesions Induced by *Leishmania amazonensis* or *Leishmania major*. *ACS Infect. Dis.* 5, 1295–1305.
- (24) Zhang, Y., Fonslow, B. R., Shan, B., Baek, M., and Yates, J. R. (2013) Protein Analysis by Shotgun/Bottom-up Proteomics. *Chem. Rev.* 113, 2343–2394.
- (25) Yi, L., Dong, N., Yun, Y., Deng, B., Ren, D., Liu, S., and Liang, Y. (2016) Chemometric methods in data processing of mass spectrometry-based metabolomics: A review. *Anal. Chim. Acta* 914, 17–34.
- (26) Ponte-Sucré, A., Gamarro, F., Dujardin, J.-C., Barrett, M. P., López-Vélez, R., García-Hernández, R., Pountain, A. W., Mwenechanya, R., Papadopoulou, B., and Maes, L. (2017) Drug resistance and treatment failure in leishmaniasis: A 21st century challenge. *PLoS Negl. Trop. Dis.* 11, No. e0006052.
- (27) Rabhi, I., Rabhi, S., Ben-Othman, R., Rasche, A., Daskalaki, A., Trentin, B., Piquemal, D., Regnault, B., Descoteaux, A., Guizani-Tabbane, L., Attia, H., Ben Miled, S., Benkahla, A., Bruno, R., Cazenave, P. A., Checkmeneva, E., Dellagi, K., Gabdoulline, R., Ghedira, K., Guerfali, F. Z., Gustin, C., Herwig, R., Hide, W., Hofmann, O., Hornischer, K., Kel, A., Kiselev, I., Kolpakov, F., Kondrakhin, Y., Kutumova, E., Land, S., Laouini, D., Lemaire, J., Liebich, I., Manchon, L., Matys, V., Michael, H., Mkannez, G., Noguier, F., Pierrat, F., Renard, P., Ryabova, A., Jauregui, S. R., Schacherer, F., Sghaier, R. M., Sharipov, R., Stegmaier, P., Tiffin, N., Tolstykh, N., Valeev, T., Voss, N., Wierling, C., and Yevshin, I. (2012) Transcriptomic Signature of *Leishmania* Infected Mice Macrophages: A Metabolic Point of View. *PLoS Neglected Trop. Dis.* 6, e1763.
- (28) Jean Beltran, P. M., Federspiel, J. D., Sheng, X., and Cristea, I. M. (2017) Proteomics and integrative omic approaches for understanding host-pathogen interactions and infectious diseases. *Mol. Syst. Biol.* 13, 922.
- (29) Beattie, L., D'El-Rei Hermida, M., Moore, J. W. J., Maroof, A., Brown, N., Lagos, D., and Kaye, P. M. (2013) A transcriptomic network identified in uninfected macrophages responding to inflammation controls intracellular pathogen survival. *Cell Host Microbe* 14, 357–368.
- (30) Lynn, M. A., Marr, A. K., and McMaster, W. R. (2013) Differential quantitative proteomic profiling of *Leishmania infantum* and *Leishmania mexicana* density gradient separated membranous fractions. *J. Proteomics* 82, 179–192.
- (31) Scorza, B., Carvalho, E., and Wilson, M. (2017) Cutaneous Manifestations of Human and Murine Leishmaniasis. *Int. J. Mol. Sci.* 18, 1296.
- (32) Rauniyar, N., and Yates, J. R., III (2014) Isobaric labeling-based relative quantification in shotgun proteomics. *J. Proteome Res.* 13, 5293–309.
- (33) Moretti, F., Bergman, P., Dodgson, S., Marcellin, D., Claerr, I., Goodwin, J. M., Dejesus, R., Kang, Z., Antczak, C., Begue, D., Bonenfant, D., Graff, A., Genoud, C., Reece-Hoyes, J. S., Russ, C., Yang, Z., Hoffman, G. R., Mueller, M., Murphy, L. O., Xavier, R. J., et al. (2018) TMEM41B is a novel regulator of autophagy and lipid mobilization. *EMBO Rep.* 19, No. e45889.
- (34) Morita, K., Hama, Y., and Mizushima, N. (2019) TMEM41B functions with VMP1 in autophagosome formation. *Autophagy* 15, 922–923.
- (35) Burdette, D. L., Monroe, K. M., Sotelo-Troha, K., Iwig, J. S., Eckert, B., Hyodo, M., Hayakawa, Y., and Vance, R. E. (2011) STING is a direct innate immune sensor of cyclic di-GMP. *Nature* 478, 515–518.
- (36) Pagliarini, D. J., Calvo, S. E., Chang, B., Sheth, S. A., Vafai, S. B., Ong, S.-E., Walford, G. A., Sugiana, C., Boneh, A., Chen, W. K., Hill, D. E., Vidal, M., Evans, J. G., Thorburn, D. R., Carr, S. A., and Mootha, V. K. (2008) A Mitochondrial Protein Compendium Elucidates Complex I Disease Biology. *Cell* 134, 112–123.
- (37) Kane, M. M., and Mosser, D. M. (2001) Progression in Leishmaniasis The Role of IL-10 in Promoting Disease. *J. Immunol.* 166, 1141–1147.
- (38) Hishikawa, D., Shindou, H., Kobayashi, S., Nakanishi, H., Taguchi, R., and Shimizu, T. (2008) Discovery of a lysophospholipid acyltransferase family essential for membrane asymmetry and diversity. *Proc. Natl. Acad. Sci. U. S. A.* 105, 2830–2835.
- (39) Merida-De-Barros, D. A., Chaves, S. P., Belmiro, C. L. R., and Wanderley, J. L. M. (2018) Leishmaniasis and glycosaminoglycans: a future therapeutic strategy? *Parasites Vectors* 11, 536.
- (40) Vázquez-Mendoza, A., Carrero, J. C., and Rodríguez-Sosa, M. (2013) Parasitic Infections: A Role for C-Type Lectins Receptors. *BioMed Res. Int.* 2013, 456352.
- (41) Huttlin, E. L., Jedrychowski, M. P., Elias, J. E., Goswami, T., Rad, R., Beausoleil, S. A., Villén, J., Haas, W., Sowa, M. E., and Gygi, S. P. (2010) A Tissue-Specific Atlas of Mouse Protein Phosphorylation and Expression. *Cell* 143, 1174–1189.
- (42) Mootha, V. K., Bunkenborg, J., Olsen, J. V., Hjerrild, M., Wisniewski, J. R., Stahl, E., Bolouri, M. S., Ray, H. N., Sihag, S., Kamal, M., Patterson, N., Lander, E. S., and Mann, M. (2003) Integrated Analysis of Protein Composition, Tissue Diversity, and Gene Regulation in Mouse Mitochondria. *Cell* 115, 629–640.
- (43) Mmp12 - Macrophage metalloelastase precursor - Mus musculus (Mouse) - Mmp12 gene and protein.
- (44) Lsm1 - U6 snRNA-associated Sm-like protein LSm1 - Mus musculus (Mouse) - Lsm1 gene and protein.

- (45) Kumar, S., Boehm, J., and Lee, J. C. (2003) p38 MAP kinases: key signalling molecules as therapeutic targets for inflammatory diseases. *Nat. Rev. Drug Discovery* 2, 717–726.
- (46) Mosser, D. M., and Zhang, X. (2008) Activation of murine macrophages. *Curr. Protoc. Immunol.* 83 (1), 14.2.1–14.2.8.
- (47) Cardiff, R. D., Miller, C. H., and Munn, R. J. (2014) Manual hematoxylin and eosin staining of mouse tissue sections. *Cold Spring Harb. Protoc.* 2014, 655–658.
- (48) Eng, J. K., McCormack, A. L., and Yates, J. R. (1994) An approach to correlate tandem mass spectral data of peptides with amino acid sequences in a protein database. *J. Am. Soc. Mass Spectrom.* 5, 976–989.
- (49) Cociorva, D., Tabb, D. L., and Yates, J. R. (2007) Validation of Tandem Mass Spectrometry Database Search Results Using DTASelect. *Current Protocols in Bioinformatics* 16, 13.4.1–13.4.14.
- (50) Elias, J. E., and Gygi, S. P. (2007) Target-decoy search strategy for increased confidence in large-scale protein identifications by mass spectrometry. *Nat. Methods* 4, 207–214.
- (51) Park, S. K., Venable, J. D., Xu, T., and Yates, J. R. (2008) A quantitative analysis software tool for mass spectrometry-based proteomics. *Nat. Methods* 5, 319–322.
- (52) Xia, J., and Wishart, D. S. (2016) Using MetaboAnalyst 3.0 for Comprehensive Metabolomics Data Analysis. *Current Protocols in Bioinformatics* 55, 14.10.1–14.10.91.
- (53) Schneider, C. A., Rasband, W. S., and Eliceiri, K. W. (2012) NIH Image to ImageJ: 25 years of image analysis. *Nat. Methods* 9, 671–675.